Targeting the platelet-derived growth factor receptor α with a neutralizing human monoclonal antibody inhibits the growth of tumor xenografts: Implications as a potential therapeutic target

Nick Loizos, Yan Xu, Jim Huber, Meilin Liu, Dan Lu, Bridget Finnerty, Robin Rolser, Asra Malikzay, Anita Persaud, Erik Corcoran, Dhanvanthri S. Deevi, Paul Balderes, Rajiv Bassi, Xenia Jimenez, Christopher J. Joynes, Venkata R.M. Mangalampalli, Philipp Steiner, James R. Tonra, Yan Wu, Daniel S. Pereira, Zhenping Zhu, Dale L. Ludwig, Daniel J. Hicklin, Peter Bohlen, Larry Witte, and Paul Kussie

ImClone Systems Incorporated, New York, New York

Abstract

Platelet-derived growth factor receptor α (PDGFRα) is a type III receptor tyrosine kinase that is expressed on a variety of tumor types. A neutralizing monoclonal antibody to human PDGFRα, which did not cross-react with the β form of the receptor, was generated. The fully human antibody, termed 3G3, has a K_d of 40 pmol/L and blocks both PDGF-AA and PDGF-BB ligands from binding to PDGFRα. In addition to blocking ligand-induced cell mitogenesis and receptor autophosphorylation, 3G3 inhibited phosphorylation of the downstream signaling molecules Akt and mitogen-activated protein kinase. This inhibition was seen in both transfected and tumor cell lines expressing PDGFRα. The *in vivo* antitumor activity of 3G3 was tested in human glioblastoma (U118) and leiomyosarcoma (SKLMS-1) xenograft tumor models in athymic nude mice. Antibody 3G3 significantly inhibited the growth of U118 ($P = 0.0004$) and SKLMS-1 ($P < 0.0001$) tumors relative to control. These data suggest that 3G3 may be useful for the treatment of tumors that express PDGFRα. [Mol Cancer Ther 2005;4(3):369–79]

Introduction

Platelet-derived growth factor receptor α (PDGFRα) is a receptor tyrosine kinase that can be activated by PDGF-AA, PDGF-AB, PDGF-BB, and PDGF-CC (1, 2). These growth factors are dimeric molecules composed of disulfide-linked polypeptide chains that bind to two receptors simultaneously and induce receptor dimerization, autophosphorylation, and intracellular signaling. PDGFRα can form homodimers as well as heterodimers with the structurally similar PDGFRβ. Given that PDGFRβ does not bind the PDGF-A chain with high affinity, PDGF-AA activates only αα receptor dimers, PDGF-AB and PDGF-CC activates αα and αβ receptor dimers, and PDGF-BB activates all three combinations of receptor dimers.

A critical role for PDGFRα during early development is evident by the fact that mice homozygous for a null mutation die during embryogenesis. The homozygotes exhibit cranial malformations and a deficiency in myotome formation (3). At later stages of development, PDGFRα is expressed in many mesenchymal structures, whereas adjacent epithelial cells produce PDGFs (reviewed in ref. 4). In the adult, PDGFs function in wound healing by activating mitogenesis, chemotaxis, and protein synthesis of PDGFR-positive fibroblasts and smooth muscle cells (5). Although these mesenchymal cells are considered to be the ''classic'' targets for PDGFs, tumor cells have also been shown to express PDGFRs. Tumors reported to express PDGFRα include but are not limited to ovarian (6), prostate (7), breast (8), lung (9), glioma (10), melanoma (11), and bone (12). Coexpression of PDGFs and PDGFRα in certain tumor types (e.g., ref. 6), consistent with autocrine growth, and overexpression of PDGFRα in certain cancer cells (13) provide evidence for the involvement of this receptor in tumorigenesis.

The recently approved drug Herceptin has validated the approach of targeting receptor tyrosine kinases present on tumor cells in the treatment of cancer (14). Indeed, Gleevec inhibits PDGFRs and is being tested in clinical trials as a treatment for PDGFRα-expressing prostate tumors (15). Neutralizing antibodies to PDGFRα have been reported previously (16, 17) and shown to inhibit the growth of cancer cells *in vitro* (16).

This study focuses on generating an antibody to PDGFRα that blocks ligand activation and testing its affect on tumor growth *in vivo*. A neutralizing antibody, designated 3G3, was shown to have antimitogenic activity on tumor cells *in vitro* and antitumor growth activity on human xenografts *in vivo*. The potential for treating a malignancy with an antibody targeting PDGFRα-expressing tumor and/or stromal cells will be discussed.

Materials and Methods

Reagents and Cell Lines

Human PDGFRα extracellular domain (ECD) and a neutralizing mouse monoclonal antibody (mAb) to human

Received 4/29/04; revised 12/1/04; accepted 12/28/04.

The costs of publication of this article were defrayed in part by the payment of page charges. This article must therefore be hereby marked advertisement in accordance with 18 U.S.C. Section 1734 solely to indicate this fact.

Requests for reprints: Nick Loizos, Department of Protein Chemistry, ImClone Systems, Inc., 180 Varick Street, New York, NY 10014. Phone: 646-638-5015; Fax: 212-645-2054. E-mail: NickL@Imclone.com

PDGFRα were purchased from R&D Systems (Minneapolis, MN). Human PDGF-AA and PDGF-BB were from Austral Biologicals (San Ramon, CA). [^{125}I]PDGF-AA (specific activity of 4,500 Ci/mmol) and [^{125}I]PDGF-BB (specific activity of 1,400 Ci/mmol) were purchased from Biomedical Technologies (Stoughton, MA) and Perkin-Elmer (Boston, MA), respectively. PDGF-AA was also iodinated to a specific activity of 1,500 Ci/mmol with iodo-beads from Pierce (Rockford, IL) and ^{125}I (specific activity of 17.4 Ci/mg) from Perkin-Elmer. [^{3}H]Thymidine was from ICN (Irvine, CA). Antibodies to phosphotyrosine were from Calbiochem (San Diego, CA) and a polyclonal anti-PDGFR-A/B antibody was purchased from Upstate Biotechnology (Lake Placid, NY). Antibodies to phospho-p44/p42 mitogen-activated protein kinase (MAPK) and p44/p42 MAPK were from Cell Signaling (Beverly, MA). An antibody to phospho-Akt (pSer$^{472/473/474}$) was from BD Biosciences (San Diego, CA). Peroxidase-conjugated protein A was purchased from Calbiochem. Dr. C-H. Heldin (Ludwig Institute for Cancer Research, Uppsala, Sweden) provided porcine aortic endothelial cells stably expressing PDGFRα (PAE Rα; ref. 18). This line was grown in F-12 medium with 10% fetal bovine serum and 0.1 mg/mL G418. U118 and SKLMS-1 cells were obtained from the American Type Culture Collection (Rockville, MD) and grown in DMEM plus 10% fetal bovine serum.

Antibody Production

Transgenic mice coding for fully human antibodies (Medarex, Inc., Sunnyvale, CA) were immunized i.p. with 3×10^7 PAE Rα cells. After 4 weeks, mice were boosted s.c. with 50 μg PDGFRα ECD in complete Freund's adjuvant plus 3×10^7 PAE Rα cells given i.p. Mice were boosted two more times, 3 weeks apart, with 25 μg PDGFRα ECD in incomplete Freund's adjuvant. Splenocytes from mice with high serum binding and blocking titers (see Receptor Binding and Ligand Blocking Assays) were isolated and fused with myeloma cells by standard procedures (19). Sixty percent of the supernatants from 1,294 hybridoma cultures showed PDGFRα binding activity and 3.4% (n = 44) blocked ligand binding the receptor to background levels in the blocking assay. Hybridoma cultures displaying blocking activity were subcloned and antibodies from these hybridomas were purified by protein G chromatography.

Phage display library–derived antibodies were obtained by selection of a human naive phage display Fab library (20) on recombinant PDGFRα ECD protein following a protocol described previously (21). A total of three round selections were carried out on immobilized receptor protein: 53 of 93 (57%) randomly picked clones after the second round selection and 84 of 93 (90%) clones after the third round selection showed PDGFRα binding activity. Among these binders, 40 (29%) clones also showed various activities in blocking the PDGF/PDGFRα interaction (defined as ≥50% inhibition of ligand binding to receptor). DNA fingerprinting and sequencing analysis of these 40 blockers revealed 11 unique antibody sequences. Two best blockers, 2D1 and 3H9, after being converted into full-length IgG format, showed receptor binding affinity of 2.7 and 0.26 nmol/L as determined by BIAcore analysis, respectively. Further affinity maturation of 3H9 via a chain-shuffling approach (22) led to the identification of clone F12 with much enhanced binding affinity (70 pmol/L) and blocking activity (see Table 1; Figs. 1 and 2).

Phage-derived Fabs were made into full-length IgGs and expressed in COS or NS0 cells as described (23). Full-length IgG1 antibody was purified by protein A affinity chromatography (Poros A, PerSeptive Biosystems, Inc., Foster City, CA).

Receptor-Binding and Ligand-Blocking Assays

Fabs and IgGs were evaluated for binding to PDGFRα in a direct binding assay. Specifically, PDGFRα ECD in PBS was immobilized onto a 96-well plate (100 ng/well). Plates were then washed with PBST (PBS + 0.05% Tween 20) and blocked with PBSM (3% milk in PBS, 200 μL/well) for 2 hours at 25°C. Fabs or IgGs were diluted in PBSM and transferred to the 96-well plate. After a 1-hour incubation at 25°C, the plates were washed with PBST and the secondary antibody (1:5,000 diluted in PBSM) was added for 1 hour at 25°C. The secondary antibody was a goat F(ab′)2 anti-human IgG-horseradish peroxidase conjugate (BioSource International, Camarillo, CA). After plates were washed with PBST, a TMB peroxidase substrate (KPL, Gaithersburg, MD) was added and the reaction was stopped with 100 μL of 1 mol/L H_2SO_4. Plates were read at $A_{450\ nm}$ using a microplate reader (Molecular Devices, Sunnyvale, CA).

Table 1. PDGFRα binding analysis of anti-PDGFRα mAbs

mAb	PDGFRα binding* (ED_{50}, nmol/L)	PDGF blocking†		Binding kinetics‡		
		Solid phase (IC_{50}, nmol/L)	Cell based (IC_{50}, nmol/L)	K_{on} (10^5 mol/L^{-1} s^{-1})	K_{off} (10^{-4} s^{-1})	K_d (10^{-9} mol/L)
3G3	0.06	0.24	0.58	11.50	0.47	0.04
7C3	0.22	0.28	0.88	3.21	0.79	0.25
7G11	0.25	0.68	3.04	8.16	0.95	0.12
16G5	1.08	0.91	4.97	1.28	2.08	1.62
F12	0.06	0.16	0.51	59.20	4.00	0.07

*Determined by direct binding ELISA. Numbers represent mAb concentrations that give 50% of maximum binding (see also Fig. 1A).
†Numbers represent mAb concentrations that give 50% inhibition of PDGF-AA binding to immobilized and cell-surface receptor (see also Fig. 1B and C).
‡Determined by BIAcore analysis.

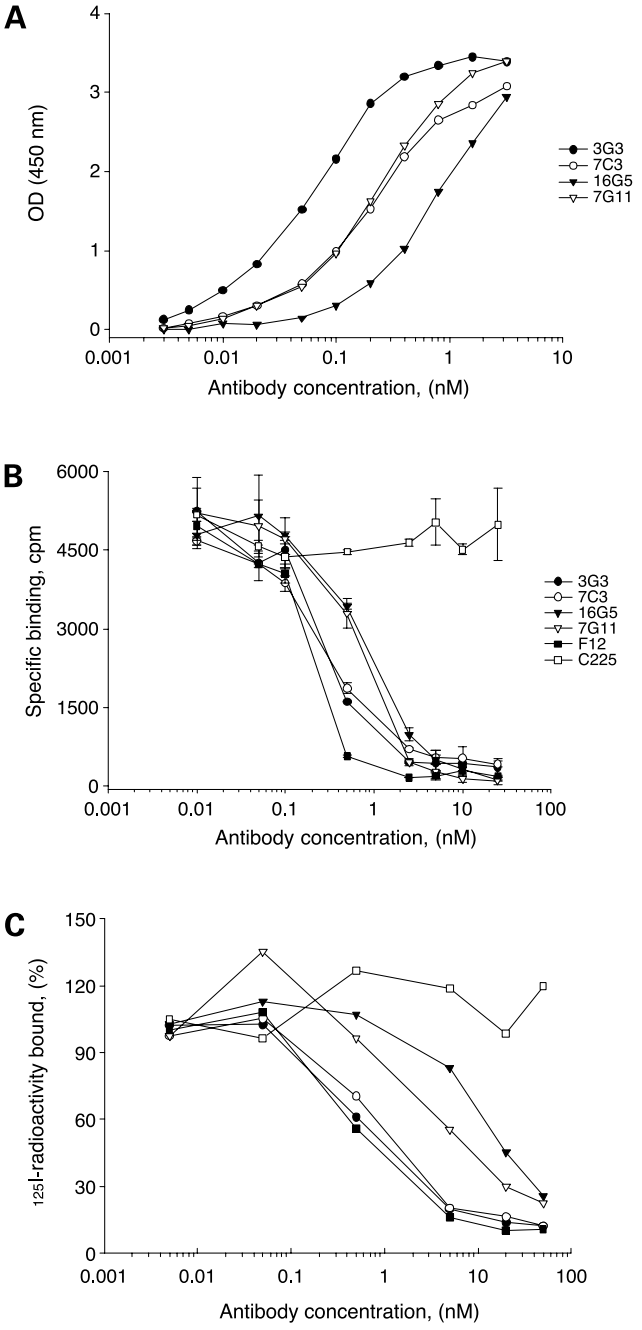

Figure 1. Binding of human antibodies to the human PDGFRα. **A,** direct binding of mAbs to immobilized PDGFRα. Binding curve for the F12 antibody is not shown (see Table 1 for ED_{50}). **B,** inhibition of [^{125}I]PDGF-AA binding to immobilized PDGFRα by mAbs. mAbs were preincubated with well-coated PDGFRα after which [^{125}I]PDGF-AA was added and its binding was measured. Specific binding was obtained by subtracting nonspecific binding ([^{125}I]PDGF-AA binding to the well in the absence of coated receptor, ~300 cpm) from total binding of each sample. *Points,* average of duplicate samples; *bars,* SD. **C,** inhibition of [^{125}I]PDGF-AA binding to cell-surface PDGFRα. Binding of [^{125}I]PDGF-AA to PAE Rα cells incubated at 0°C was determined in the presence of increasing amounts of mAbs. Binding in the absence of mAbs was set at 100%. Same legend symbols for **B** and **C**. Anti–epidermal growth factor receptor antibody C225 (ImClone Systems, Inc., New York, NY) serves as a negative control for experiments done throughout the study.

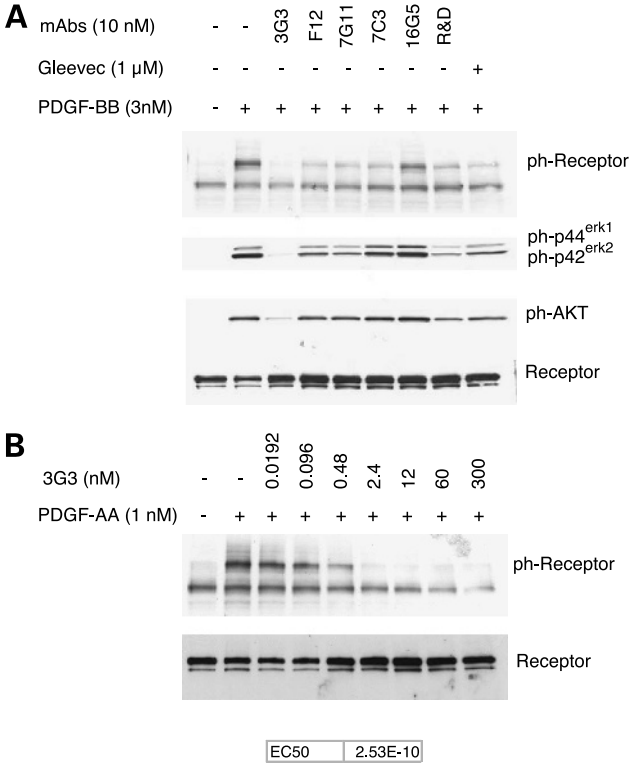

Figure 2. Specific inhibition of PDGFRα phosphorylation and that of downstream-effector molecules by mAbs. **A,** PAE Rα cells were rendered quiescent, treated with mAbs, and then stimulated with either PDGF-AA or PDGF-BB (1 and 3 nmol/L, respectively) for 10 min. Afterward, cell lysates were analyzed by SDS-PAGE and Western blotting with anti-phosphotyrosine, anti-phospho-MAPK, and anti-phospho-Akt antibodies. An equal amount of loaded sample per gel lane was determined by probing for PDGFRα. Gleevec and a neutralizing mouse mAb were included in these experiments as positive control inhibitors. **B,** titration of the inhibitory affect for mAb 3G3 on PDGFRα autophosphorylation and its EC_{50} (3G3 molar concentration required for 50% inhibition of receptor phosphorylation).

Phage were also screened for PDGFRα binding in this assay modified by (*a*) preincubating the phage in PBSM for 2 hours to block nonspecific binding and (*b*) using an anti–M13 phage-horseradish peroxidase conjugate (Amersham Biosciences, Piscataway, NJ) as the secondary antibody.

A solid-phase PDGF blocking assay was adapted from Duan et al. (24). Specifically, PDGFRα ECD was diluted in PBS and coated on 96-well microtiter plates. Plates were made with Immulon 2HB flat-bottomed 1 × 12 Removawell strips of irradiated protein binding polystyrene (Dynex Technologies, Chantilly, VA). Each well was coated with 60 ng PDGFRα for 3 hours at 25°C in a total volume of 100 μL. Plates were then washed twice and blocked overnight at 4°C with 25 mmol/L HEPES (pH 7.45), 0.5% gelatin, 100 mmol/L NaCl, and 0.1% Tween 20. Plates were then warmed to 25°C for 20 minutes and washed once with binding buffer [25 mmol/L HEPES (pH 7.45), 0.3% gelatin, 100 mmol/L NaCl, 0.01% Tween 20]. Fifty microliters of phage, Fabs, or IgGs were added to each well and

incubated at 25°C for 30 minutes. Iodinated PDGF was diluted in binding buffer and added (50 μL of a 1 nmol/L solution) to each well. Plates were incubated for 2 hours at 25°C and then washed five times with binding buffer. Each well was counted in a gamma counter. A cell-based blocking assay was done as described (25).

BIAcore Analysis

The binding kinetics of antibodies to PDGFRα was measured using a BIAcore 3000 instrument (BIAcore, Inc., Piscataway, NJ). PDGFRα ECD was immobilized onto a sensor chip and antibody was injected at various concentrations. Sensograms were obtained at each concentration and evaluated using the BIA Evaluation 2.0 program to determine the rate constants. The affinity constant, K_d, was calculated from the ratio of rate constants K_{off}/K_{on}.

Antimitogenic Assay

Cells were seeded in 96-well tissue culture plates (1×10^4 cells per well) and grown overnight in 100 μL medium per well. The wells were then rinsed with serum-free medium and cells were serum starved overnight with 75 μL serum-free medium added to each well. IgGs were added (25 μL/well) and the plates were incubated for 30 minutes at 37°C. PDGF-AA or PDGF-BB (25 μL/well) was then added and plates were incubated for 18 to 20 hours at 37°C. Plates were incubated for an additional 4 hours after each well received 0.25 μCi [^{3}H]thymidine (25 μL/well). Antibodies, PDGF, and [^{3}H]thymidine were all diluted in serum-free medium. Cells were then washed with PBS plus 1% bovine serum albumin and detached by treatment with trypsin (100 μL/well). The cells were collected onto a filter and washed thrice with double-distilled water using a MACH III cell harvester (Tomtec, Inc., Hamden, CT). After processing the filter, DNA incorporated radioactivity was determined on a scintillation counter (Wallac Microbeta, model 1450).

Phosphorylation Assays

Receptor and downstream signaling molecule phosphorylation assays were done as described (24). Briefly, cells were seeded in six-well Falcon tissue culture plates (250,000 cells per well) and allowed to grow overnight. Wells were then rinsed and incubated in serum-free medium. After an overnight incubation to render cells quiescent, the cells were treated with antibodies for 30 minutes at 37°C followed by adding PDGF-AA or PDGF-BB and incubating for an additional 10 minutes at 37°C. Cells were then detached and lysed in 200 μL lysis buffer [50 mmol/L Tris-HCl (pH 8.0), 1% Triton X-100, 150 mmol/L NaCl, 1 mmol/L EDTA, 0.1% SDS, 1 mmol/L sodium orthovanadate, and protease inhibitors (Complete Mini, Roche, Mannheim, Germany)]. Cell lysates were analyzed by SDS-PAGE and Western blotting using enhanced chemiluminescence reagents and Hyperfilm (Amersham Biosciences).

Flow Cytometry

Adherent tumor and normal cells were grown to near confluence and released using cell dissociation buffer (Sigma, St. Louis, MO). Cells were then washed in PBS, resuspended in buffer A (PBS + 1% bovine serum albumin), and filtered. Test tubes received 1×10^6 cells in 100 μL buffer A and were stained with a mouse anti-human PDGFRα antibody at a concentration of 2.5 μg/mL. After a 1-hour incubation on ice, cells were washed in buffer A and incubated with a goat anti-mouse IgG-fluorescein conjugate (BioSource International) in 100 μL buffer A at 7 μg/mL for 1 hour on ice. Control samples were stained only with this secondary antibody. All samples were analyzed using a FACSvantage SE flow cytometer (BD Biosciences).

Direct Binding of ^{125}I-Labeled Antibody to PDGFRα-Expressing Tumor Cells and Scatchard Plot Analysis

mAb 3G3 was radiolabeled with ^{125}I as described for PDGF-AA (see above) and retained the same PDGFRα binding activity as unlabeled 3G3 in a solid-phase assay (data not shown). U118 and SKLMS-1 cells were seeded in 12-well Costar plates (100,000 cells per well) and incubated with 2-fold serial dilutions of [^{125}I]3G3 starting at 66 ng/mL. Incubations were done for 2 hours at 4°C. As a control for nonspecific cell association of radioactivity, cell binding was done in the presence of a 200-fold excess of unlabeled 3G3. Data were analyzed using Sigma Plot version 8.02 software to obtain the K and an estimate of the maximal number of mAbs bound per cell.

Treatment of Subcutaneous Xenografts in Nude Mice

All animal studies were conducted according to U.S. Department of Agriculture and NIH guidelines and approved by an Institutional Animal Care and Use Committee. S.c. tumor xenografts were established by injecting 10×10^6 SKLMS-1 or U118 cells mixed in Matrigel (Collaborative Research Biochemicals, Bedford, MA) into female athymic nude mice (Crl:NU/NU-nuBR, Charles River Laboratories, Wilmington, MA). Tumors were allowed to reach a mean tumor volume (π / 6 × longest length × perpendicular width^2) of ~400 mm^3 and mice were randomized into five groups (n = 12). Mice were then treated by i.p. injection twice weekly for the duration of the study. Group 1 mice were treated with vehicle control (0.9% NaCl, USP for Irrigation, B/Braun). Groups 2 to 4 mice were treated with 6, 20, and 60 mg/kg 3G3, respectively. Group 5 mice were treated with 60 mg/kg human IgG (Sigma). Groups treated with 6, 20, or 60 mg/kg 3G3 or human IgG were given 21.4, 71.4, and 214 mg/kg loading doses, respectively. Loading doses were predicted to bring the plasma concentration to steady state with the first dose using single-dose pharmacokinetic values for 3G3 (elimination half-life, 7 days) and a dosing regimen of twice weekly. Tumor volumes were evaluated twice weekly. Tumor growth in the treatment groups was compared with a repeated-measures ANOVA.

For H&E staining, resected tumors were fixed in QDL fixative at 4°C for 24 hours. After paraffin embedding and sectioning at 4 μm, formalin-fixed sections were stained with Mayer's H&E (Richard Allen, Kalamazoo, MI).

For experiments examining the level of receptor phosphorylation *in vivo*, mice with established U118

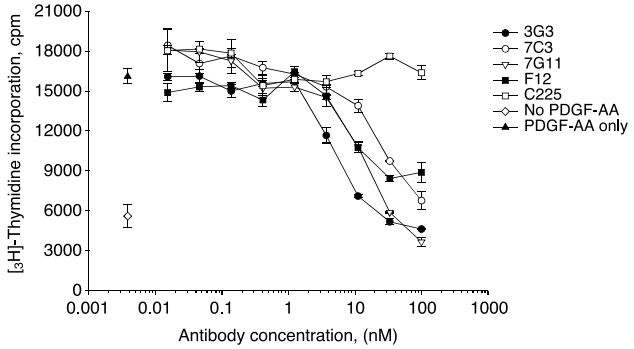

	3G3	7C3	7G11	F12
EC50	8.27E-09	2.58E-08	1.40E-08	1.42E-08

Figure 3. Inhibition of PDGF-AA-stimulated [^{3}H]thymidine incorporation in PAE Rα cells by mAbs. PAE Rα cells (1×10^4 per well) were plated into 96-well tissue culture plates and rendered quiescent. Following a 30-min preincubation with mAbs, cells were stimulated with 1 nmol/L PDGF-AA. After a 20-h incubation, 0.25 μCi [^{3}H]thymidine was added to each well and incubated for an additional 4 h. DNA incorporated radioactivity was determined with a scintillation counter. *Points,* mean of duplicate samples; *bars,* SD. Molar concentration of mAb for half-maximal inhibition of [^{3}H]thymidine incorporation induced by PDGF-AA was calculated using the program Prism (*bottom*).

tumors (500 mm^3) were treated with a 214 mg/kg loading dose followed 72 hours later by a 60 mg/kg maintenance dose of antibody. Tumors were harvested 1 week (168 hours) after the first injection of antibody and homogenized in phosphorylation assay lysis buffer (see above). The lysates were centrifuged twice at 14,000 rpm and the protein concentration for the collected supernatant was determined (Bio-Rad protein assay, Bio-Rad, Hercules, CA). Lysate (4 mg) from each sample was subject to immunoprecipitation using 3G3. Immunoprecipitated human PDGFRα was then immunoblotted as described above (see Phosphorylation Assays).

Results

Binding and Blocking Activity of mAbs

Human mAbs to the extracellular region of PDGFRα were derived from mouse transgenic (IgGs; 3G3, 7C3, 16G5, and 7G11) and phage display (IgG; F12) systems (see Materials and Methods). These mAbs were tested for binding to PDGFRα in a direct binding ELISA and on a BIAcore instrument (Table 1; Fig. 1A). Figure 1A shows dose-dependent binding of the mAbs to immobilized PDGFRα ECD in the ELISA. The antibody concentrations required for 50% maximum binding to PDGFRα ECD ranged from 0.06 to 1.08 nmol/L (Table 1). These ED_{50}s are consistent with the K_ds for the antibodies as determined by surface plasmon resonance on a BIAcore instrument (Table 1, compare 0.06 nmol/L ED_{50} versus 0.04 nmol/L K_d for mAb 3G3). Fluorescence-activated cell sorting analysis showed that all mAbs were able to bind cell-surface receptors expressed on transfected PAE Rα cells (data not shown).

The two antibodies with the highest affinity for PDGFRα also showed the best blocking activity in both solid-phase and cell-based ligand binding assays. Specifically, mAbs 3G3 and F12 inhibited [^{125}I]PDGF-AA binding to immobilized receptor with IC_{50}s of 0.24 and 0.16 nmol/L, respectively (Fig. 1B). In the cell-based assay, 3G3 and F12 inhibited [^{125}I]PDGF-AA binding to PAE Rα-expressing cells with IC_{50}s of 0.58 and 0.51, respectively (Table 1; Fig. 1C). All mAbs also blocked [^{125}I]PDGF-BB binding to immobilized receptor, with 3G3 and F12 having the lowest IC_{50}s of 0.43 and 0.55 nmol/L, respectively (data not shown). Given that the binding sites for PDGF-AA and PDGF-BB on PDGFRα are not structurally coincident (26), data suggest that the epitopes for 3G3 and F12 spatially overlap the two growth factor binding sites.

mAbs Inhibit Receptor Phosphorylation and Activation of Downstream-Effector Molecules

The effects on PDGF-induced intracellular signaling by the anti-PDGFRα antibodies were determined using PAE Rα cells. An early event in the signaling process is receptor autophosphorylation; therefore, all mAbs were tested for their ability to inhibit ligand-induced receptor tyrosine phosphorylation. PDGF-AA and PDGF-BB increase PDGFRα tyrosine phosphorylation ~5-fold at 1 and 3 nmol/L concentrations, respectively. Higher concentrations of ligand (10 nmol/L) resulted in less phosphorylated receptor possibly due to ligand-induced degradation (data not shown). Although all antibodies showed some inhibition, mAb 3G3 inhibited PDGF-BB-induced receptor phosphorylation to near background levels (Fig. 2A, *top row*). Similar data were obtained using PDGF-AA to induce receptor phosphorylation (data not shown).

PDGFs transduce mitogenic signals and exert antiapoptotic effects on receptor-expressing cells. Phosphorylations of MAPKs p44/p42 and Akt are necessary steps in cell growth and antiapoptotic pathways, respectively, and are downstream of ligand-induced receptor phosphorylation (1). All mAbs were therefore tested for their ability to inhibit the activation of these downstream-effector molecules. As can be seen in Fig. 2A, mAb 3G3 was the best inhibitor of the antibodies at lowering the phosphorylation state for both MAPKs and Akt in response to PDGF-BB. mAb 3G3 was equally as effective at inhibiting downstream-effector molecule phosphorylation when the cells were stimulated with PDGF-AA (data not shown). Inhibition of PDGFRα phosphorylation by 3G3 was dose dependent, with 50% inhibition achieved at 0.25 nmol/L (Fig. 2B).

mAbs Inhibit Ligand-Induced Cell Mitogenesis

All mAbs were tested for their ability to block PDGF-AA-induced mitogenesis of PAE Rα cells. When mAbs were added to serum-starved PAE Rα cells, PDGF-AA-induced thymidine incorporation was specifically inhibited (Fig. 3). The best antagonist was 3G3 with an EC_{50} (i.e., the antibody concentration that inhibited 50% of PDGF-AA-stimulated mitogenesis for PAE Rα cells) of 8.3 nmol/L. mAb 3G3 also inhibited the 3 nmol/L PDGF-BB-induced mitogenesis of PAE Rα cells with an EC_{50} of 1.25 nmol/L (data not shown).

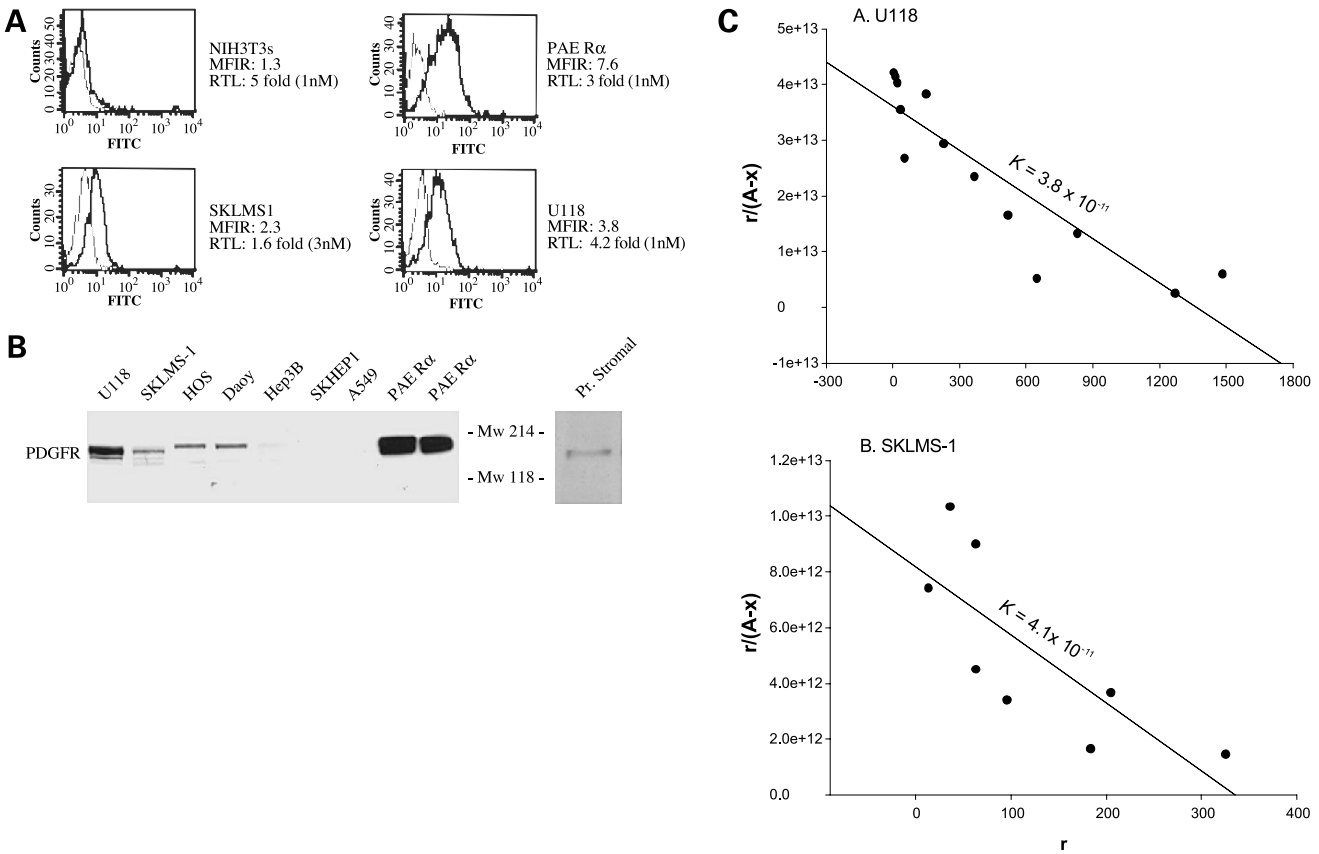

Figure 4. **A,** flow cytometric analysis of cells stained for surface expression of human PDGFRα. Control cell line expressing PDGFRα; PAE Rα cells. Control cell line not expressing human PDGFRα; NIH3T3 mouse fibroblasts. Tumor cell lines positive for PDGFRα expression; U118 and SKLMS-1. *X axis,* a measure of fluorescence intensity; *Y axis,* number of cells; *MFIR,* mean fluorescence intensity ratio [(mean fluorescence intensity of primary antibody + secondary antibody signal) / (mean fluorescence intensity of secondary antibody signal)], a relative measurement of receptor levels; *RTL,* response to ligand in a mitogenic assay. PDGF-AA concentration used to achieve the response is shown inside parentheses. NIH3T3 cells respond to ligand by virtue of expressing the mouse PDGFRα. **B,** PDGFR expression on cell lines. Cell lysates were probed for PDGFR expression by Western blotting. *Pr stromal,* prostate stromal cells. **C,** binding of ^{125}I-labeled 3G3 to U118 and SKLMS-1 cells. *r,* number of antibody molecules bound to one cell at a given dilution; *A,* molar concentration of total antibody; *x,* molar concentration of bound antibody; *A-x,* molar concentration of the free antibody. Slope of the binding curve gives the *K* (mol/L). Intersection point between the binding curve and *X* axis gives the maximum number of 3G3 molecules that can be bound to a single cell.

Tumor Cell Lines Expressing PDGFRα as Determined by Flow Cytometry and Response to Ligand Stimulation

Human tumor cell lines expressing PDGFRα were tested to determine the affects these mAbs have on inhibiting malignant growth in *in vitro* and *in vivo* systems. PDGFRα-expressing lines derived from glial tumors and sarcomas mostly have been reported (27, 28). Figure 4A shows two such tumor cell lines that express PDGFRα as seen by flow cytometry: SKLMS-1 (leiomyosarcoma) and U118 (glioblastoma). These cell lines also respond to ligand in mitogenic assays (Fig. 4A). Five other human tumor cell lines that were reported to express PDGFRα are Daoy (medulloblastoma), A549 (lung carcinoma), HOS (osteosarcoma), Hep3B, and SK-HEP-1 (liver carcinoma; refs. 9, 29, 30).[1] These cell lines were negative for receptor expression by flow cytometric analysis (data not shown). However, flow cytometry is not as sensitive as other methods (RNA analysis, immunoblotting, etc.) at detecting expression. Indeed, Daoy, HOS, and Hep3B cells were shown to express PDGFRs when screened by immunoblotting (Fig. 4B). Daoy and HOS cells did not respond to ligand in a mitogenic assay at concentrations as high as 30 nmol/L (data not shown). This lack of response could be due to a low level of expressed receptor or that PDGF-induced downstream pathways are not functional in these particular cell lines. Because SKLMS-1 and U118 cells form tumors in mice and respond to PDGF stimulation, they were chosen for further study. It should be noted that mRNA for PDGF-AA was detected in both SKLMS-1 and U118 cells and PDGF-BB mRNA was detected in only U118 cells (27, 28). However, only SKLMS-1 was shown to express PDGF-AA protein when grown in culture (data not shown) using a quantitative sandwich enzyme immunoassay

[1] S.P.S. Monga, personal communication.

technique (R&D Systems). Specifically, 106 pg/mL PDGF-AA were detected in the supernatant of nearly confluent SKLMS-1 cells with a limit of detection at ~10 pg/mL for ligands PDGF-AA, PDGF-BB, and PDGF-AB. Thus, SKLMS-1 has the potential for not only paracrine but also autocrine stimulation.

Antibody Avidity and Number of Available Epitopes on PDGFRα-Expressing Tumor Cells

A Scatchard plot analysis of direct binding for radiolabeled 3G3 to U118 and SKLMS-1 cells was done (Fig. 4C). Equilibrium constants of 3.8×10^{-11} and 4.1×10^{-11} mol/L were determined for 3G3 to U118 and SKLMS-1 cells, respectively. The results indicate that mAb 3G3 binds to U118 and SKLMS-1 cells with very similar avidity and that the *K*s determined agree with the K_ds obtained by BIAcore analysis (Table 1). The number of antibody molecules bound per U118 and SKLMS-1 cells was estimated to be 1,740 and 340, respectively, at antibody saturation. Because 3G3 is bivalent, the average number of PDGFRα molecules on these cells is likely to be 1- to 2-fold greater than the antibody number. Thus, the results indicate that there is ~5-fold less receptor on SKLMS-1 compared with U118 cells.

mAbs Inhibit Ligand-Induced Phosphorylation and Mitogenesis of Tumor Cell Lines

To determine if the anti-PDGFRα antibodies could inhibit PDGF-induced signaling in tumor cells, the phosphorylation state of downstream-effector molecules Akt and MAPKs p44/p42 was tested in their presence and absence before exogenous ligand stimulation (Fig. 5). As can be seen in Fig. 5A, mAb 3G3 was the best antagonist of the antibodies at inhibiting the phosphorylation of both Akt and MAPKs in response to PDGF-AA stimulation of SKLMS-1 cells. Comparing 3G3 with the phage-derived antibody F12 and the commercially available mouse mAb shows 3G3 to be the better inhibitor of downstream signaling in U118 cells (Fig. 5B). The inhibition of Akt phosphorylation by 3G3 was 100% and that of MAPKs was ~80% (see Fig. 5, columns for percentage inhibition for all mAbs).

mAbs 3G3 and F12 were next tested for their ability to block ligand-induced mitogenesis of tumor cells. When mAbs were added to serum-starved U118 cells, PDGF-AA-induced thymidine incorporation was specifically inhibited (Fig. 6A). The best antagonist was 3G3 with an EC_{50} of 3.4 nmol/L. mAb 3G3 has also been proven to have the greatest antagonist activity for the PDGF-AA-induced mitogenic response of SKLMS-1 cells with a 5 nmol/L EC_{50} (Fig. 6B). All mitogenic and phosphorylation data indicated 3G3 to be the best PDGFRα neutralizing antibody; therefore, it was solely used in the remaining experiments. SKLMS-1 cells have been reported to express only PDGFRα and not PDGFRβ (27) and this was confirmed by flow cytometric analysis (data not shown). Predictably, 3G3 inhibited PDGF-BB from stimulating DNA synthesis in SKLMS-1 cells (Fig. 6C). However, flow cytometric analysis of U118 cells showed expression of PDGFRβ in addition to PDGFRα (data not shown). mAb 3G3 was shown not to cross-react with PDGFRβ in a solid-phase ELISA and cell-based phosphorylation assay (data not shown). PDGFRβ can respond to PDGF-BB stimulation and that explains why only partial inhibition (40% at 66 nmol/L 3G3) is given by mAb 3G3 on U118 cells stimulated with PDGF-BB (Fig. 6D).

In vivo Efficacy of 3G3 and Inhibition of Tumor Xenograft Growth

The *in vivo* effects of 3G3 were tested in glioblastoma (U118) and leiomyosarcoma (SKLMS-1) s.c. xenograft

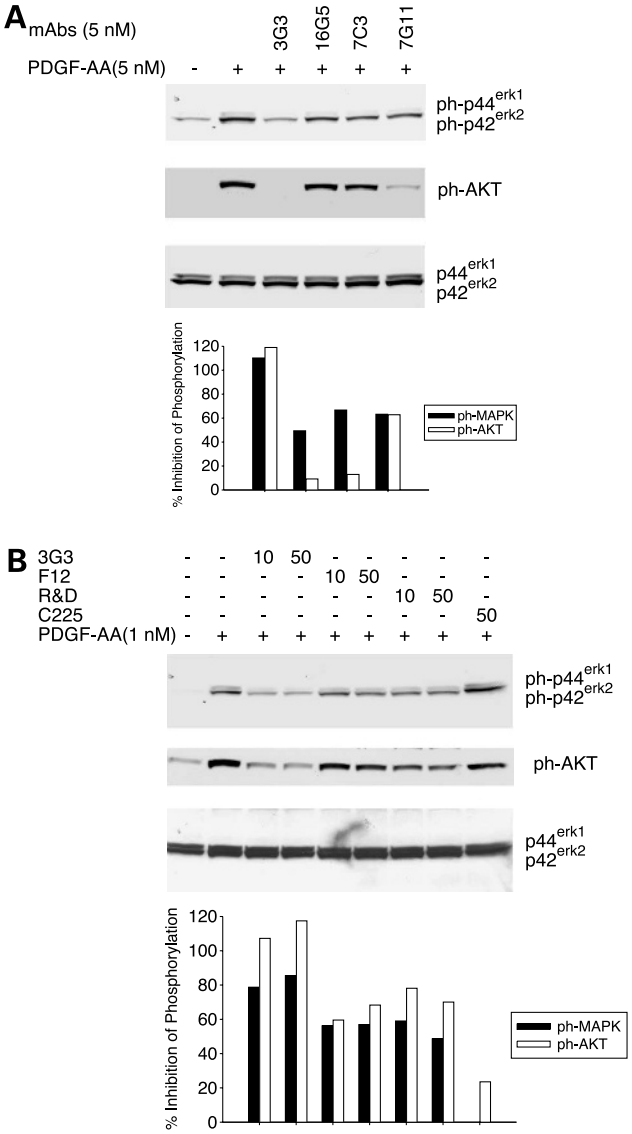

Figure 5. mAbs inhibit PDGF-AA-induced downstream-effector molecule activation. SKLMS-1 (**A**) and U118 (**B**) cells were pretreated with mAbs before stimulation with PDGF-AA. Inhibition of Akt and MAPK phosphorylation was determined by examining cell lysates through Western blotting with antibodies specific for phospho-Akt and phospho-MAPK. Percentage inhibition was calculated by {1 − [(band intensity from mAb-treated cell − band intensity from uninduced cell) / (band intensity from induced cell − band intensity from uninduced cell)]} × 100. Columns showing percentage inhibition are aligned with corresponding gel lanes. Equal loading of gel lanes was determined by Western blotting with an antibody to MAPK.

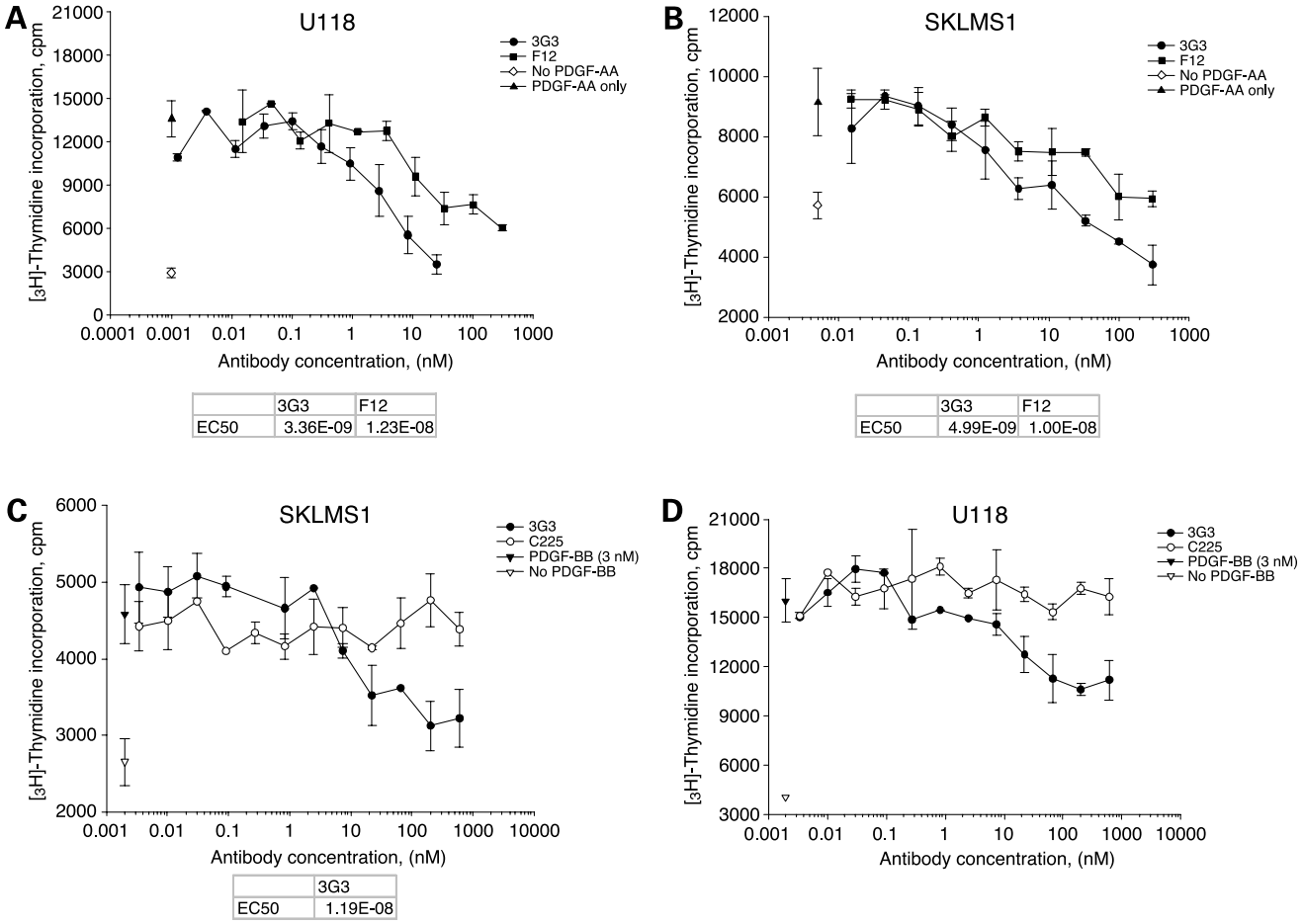

	3G3	F12
EC50	3.36E-09	1.23E-08

	3G3	F12
EC50	4.99E-09	1.00E-08

	3G3
EC50	1.19E-08

Figure 6. Inhibition of PDGF-AA-stimulated [^{3}H]thymidine incorporation in U118 (**A**) and SKLMS-1 (**B**) cells by mAbs. Tumor cells (1×10^4 per well) were plated into 96-well tissue culture plates and rendered quiescent. Following a 30-min preincubation with the mAbs, the cells were stimulated with PDGF-AA. After a 20-h incubation, 0.25 μCi [^{3}H]thymidine was added to each well and incubated for an additional 4 h. DNA incorporated radioactivity was determined with a scintillation counter. *Points,* mean of duplicate samples; *bars,* SD. Molar concentration of mAb for half-maximal inhibition of [^{3}H]thymidine incorporation induced by PDGF-AA was calculated using the program Prism (*bottom*). Inhibition of PDGF-BB-stimulated [^{3}H]thymidine incorporation in SKLMS-1 (**C**) and U118 (**D**) cells by mAb 3G3. A 3 nmol/L concentration of PDGF-BB was used to stimulate the cells.

models in athymic nude mice. Mice with established tumors (400 mm^3) were treated with 3G3, human IgG, or saline twice weekly. As shown in Fig. 7A, human IgG had no effect on glioblastoma growth compared with saline-treated mice ($P = 0.74$), whereas 3G3 significantly inhibited tumor growth at 6 ($P = 0.06$), 20 ($P = 0.03$), and 60 ($P = 0.0004$) mg/kg doses. At the end of the U118 study, the %T/C [(average tumor volume for the 3G3-treated group at conclusion of study / average tumor volume at beginning of treatment) / (average tumor volume for control-treated group at conclusion of study / average tumor volume at beginning of treatment) × 100] values were 67%, 63%, and 35% for 6, 20, and 60 mg/kg 3G3-treated dose groups, respectively. Remarkably, there were 4 of 12, 5 of 11, and 10 of 12 regressions in the 6, 20, and 60 mg/kg 3G3-treated groups, respectively, and no regressions in either control group. Figure 7B shows that leiomyosarcoma growth was also significantly inhibited by 3G3 treatment at 6 ($P = 0.02$), 20 ($P = 0.003$), and 60 ($P < 0.0001$) mg/kg. The final %T/C values were 66%, 57%, and 31% for the 6, 20, and 60 mg/kg 3G3-treated dose groups, respectively. There were no tumor regressions in this study. It should be noted that 3G3 shows no cross-reactivity to the mouse PDGFRα as determined in ELISA, mitogenic, and phosphorylation assays (data not shown). Given that 3G3 is specific to human PDGFRα, no toxicity was expected and none was observed in treated mice. Toxicity was assessed by observing for weight loss, death, and cage side observations for general health of the mice.

Histologic examination of xenografts at the end of treatment showed marked differences in tumors from animals given 3G3 compared with tumors from animals receiving control therapy. In the 60 mg/kg 3G3-treated U118 group, fewer viable tumor cells were found and there were substantially more cell-sparse regions compared with the saline-control group (Fig. 7C). SKLMS-1 xenografts at

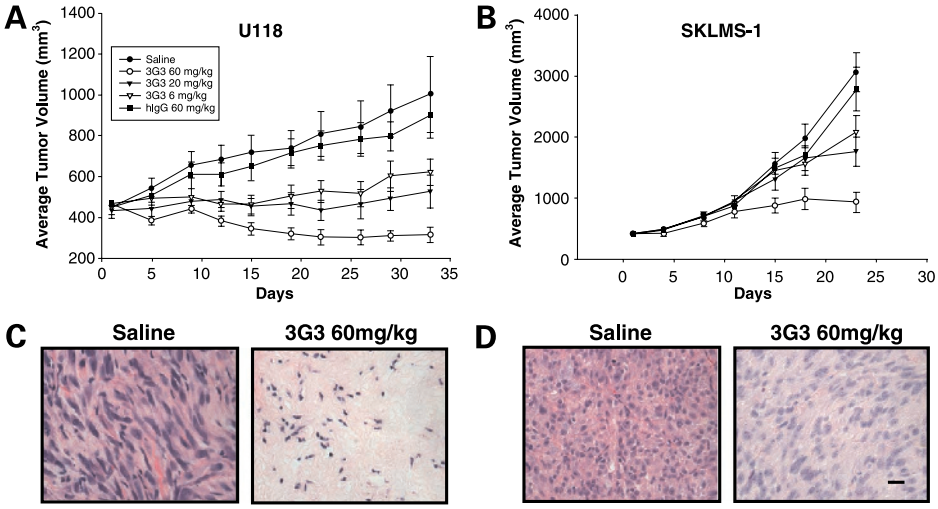

Figure 7. Growth inhibition of U118 (glioblastoma) and SKLMS-1 (leiomyosarcoma) tumor xenografts in nude mice. Dose-dependent effects for treatment of established U118 (**A**) and SKLMS-1 (**B**) tumors treated with 3G3 on a twice weekly schedule (see Materials and Methods for corresponding loading doses). Histologic examination of U118 (**C**) and SKLMS-1 (**D**) tumor xenografts (day 33 for U118 study and day 25 for SKLMS-1 study) stained with H&E. *Bar*, 20 μm.

day 25 also showed a reduction in the amount of viable tumor cells and cellular packing in the 60 mg/kg 3G3-treated group compared with the saline-control group (Fig. 7D).

mAb 3G3 Inhibits PDGFRα Stimulation in Glioblastomas

To determine whether 3G3 could modulate the activation of PDGFRα *in vivo*, the level of receptor phosphotyrosine in 'U118 tumors was evaluated 1 week after beginning 3G3 or human IgG treatment. Tumors were harvested from mice 1 week (168 hours) after the first antibody injection because this is before tumor regression is observed on average (see Fig. 7A). Human PDGFRα was immunoprecipitated from tumor extracts and immunoblotted with either an anti-PDGFR or anti-phosphotyrosine antibody. The immunoblots reveal that 3G3 treatment lowers PDGFRα phosphotyrosine levels relative to a human IgG control in these tumors (Fig. 8), thereby showing the specificity of 3G3 for PDGFRα *in vivo*.

Discussion

Several observations suggest that PDGFRα plays important roles in tumorigenesis and tumor progression. First, PDGFRα-positive cells transform by an autocrine mechanism when the *PDGF* gene or its viral counterpart, v-*sis*, is expressed (31). Coexpression of PDGFRα and PDGFs, consistent with autocrine growth, has been reported in various types of cancers (reviewed in ref. 5). Second, gene amplification and activating mutations of PDGFRα have been found in subsets of gliomas and gastrointestinal stromal tumors, respectively (13, 32). Third, PDGFRα is upregulated in medulloblastoma metastatic tumors (29). Metastasis may be increased by PDGFRα expression as shown for the mouse 3LL Lewis lung tumor (33). Additionally, paracrine stimulation of PDGFR-positive stromal cells by PDGF-BB-expressing melanoma cells enhanced xenograft growth, forming non-necrotizing

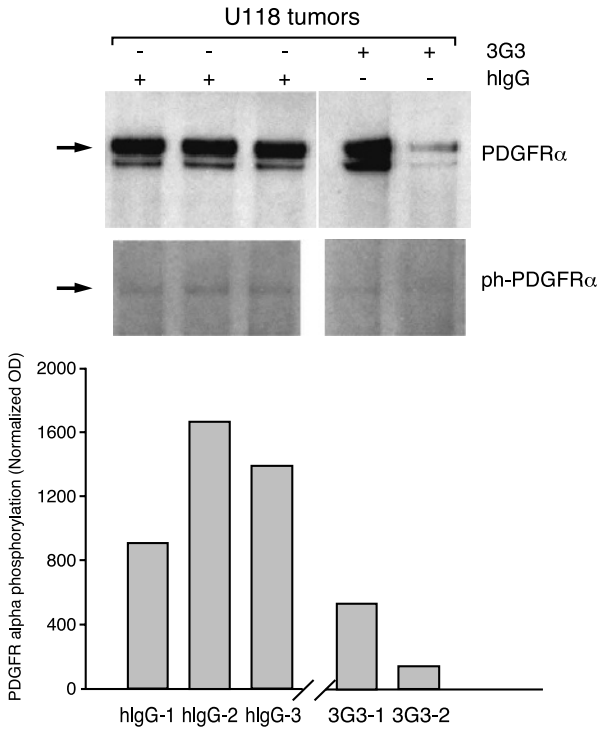

Figure 8. mAb 3G3 reduces PDGFRα phosphorylation *in vivo*. Human PDGFRα from 3G3-treated or human IgG–treated U118 tumors was immunoblotted for total and phosphorylated PDGFRα (*arrows*). Data for three tumors treated with human IgG and two tumors treated with 3G3. Data for one 3G3-treated tumor are not shown because the extracted material was less than the 4 mg required for immunoprecipitating the receptor as determined by the Bio-Rad protein assay and visualizing total extracted protein on anti-tubulin Western blots (data not shown). Scanned values for total PDGFRα were divided by the highest scanned value and the highest scanned value was then set to 1. These normalization factors were multiplied by their corresponding scanned values for phosphorylated PDGFRα to determine the normalized amount of phosphorylated PDGFRα (*bottom*). Scanned values for phosphorylated PDGFRα were each adjusted for background because some parts of the film were darker. *OD,* absorbance.

tumors with a markedly rich tissue stroma (34). By comparison, melanoma cells not directed to express PDGF-BB formed necrotizing tumors with a weak tissue stroma, thus indicating the potential importance of PDGFR-activated stromal cells in facilitating tumor formation. The individual contributions of PDGFRα and PDGFRβ were not evaluated in the study (34). Regardless, these observations justify testing cancer drugs that specifically target PDGFRα.

Targeting PDGFRα on cancer cells has been proven effective at inhibiting their proliferation in xenograft models. mAb 3G3 was more effective at inhibiting tumor growth of the U118 versus the SKLMS-1 xenografts (Fig. 7). Interestingly, U118 cells express more PDGFRα and have a greater mitogenic response to ligand than SKLMS-1 cells (Fig. 4A and C). Therefore, PDGFRα levels in xenografts may indicate the response to antibody treatment. The SKLMS-1 cells express PDGF-AA protein and thus may undergo autocrine growth (28). Importantly, a neutralizing antibody to PDGFRα has already been shown to inhibit autocrine growth in culture of PDGFRα-positive cells transfected with PDGF (16). This result may have been unexpected given that PDGF forms a complex with PDGFR within the endoplasmic reticulum of cells coexpressing both ligand and receptor (35). However, the mitogenic signals were only transmitted when the complex reached the plasma membrane, thus being susceptible to neutralizing antibodies (36). Therefore, mAb 3G3 could work on a cancer cell within a tumor by inhibiting its paracrine and autocrine stimulation. Future studies need to address whether the antibody has other effects on the cancer cell, such as the mediation of antibody-dependent cell cytotoxicity and/or receptor down-modulation. By down-modulating the receptor, 3G3 may also be effective on tumors with activating mutations in the intracellular domain of PDGFRα, such as those found in GISTs (32). mAb 3G3 should also be tested in orthotopic xenografts for prostate, ovarian, and pancreatic cancer because Gleevec has been shown to inhibit both PDGFR activation in and tumor growth of these models (37–39).

The stromal fibroblasts of many tumors, including breast, prostate, and lung, express PDGFRα, whereas the epithelial-derived carcinoma cells secrete PDGFs (7, 8, 40, 41). There are data indicating that PDGFs released by carcinoma cells activate stromal cells to express proteins important for tumor progression. For example, PDGF is reported to activate myofibroblasts to synthesize collagen, a major component of the stromal response in breast carcinoma (42). In another example, matrix metalloproteinases are expressed by PDGF-stimulated fibroblasts (43). In particular, proper matrix metalloproteinase-2 expression is believed to be dependent on PDGFRα signaling as shown in experiments examining the development of *Patch* mutant mice that contain a deletion of the receptor (44). Lastly, PDGF-BB-activated stromal cells promote the tumor development of nontumorigenic keratinocytes apparently by a paracrine mechanism (45) and melanoma cells by mediating the formation of a connective tissue framework (34). Future *in vitro* and *in vivo* studies using commingled human stromal and tumor cells would help to determine if 3G3 inhibition of PDGFRα activation can lower the tumor-promoting activity of stromal cells. Such studies are needed given that 3G3 does not cross-react with the mouse PDGFRα.

In conclusion, a potent neutralizing antibody to PDGFRα has been generated and shown to be effective at inhibiting the growth of PDGFRα-expressing xenografts in nude mice. *In vitro* studies showed the antibody can inhibit receptor signaling in cancer cells. Future studies are needed to determine what other effects 3G3 treatment has on cancer and tumor stromal cells. In addition, this mAb should be useful in distinguishing the contributions of PDGFRα and PDGFRβ in pericyte recruitment (46) and interstitial fluid pressure homeostasis (47), as these processes have only been investigated with small molecule inhibitors that target both receptors.

Acknowledgments

We thank Dr. C-H. Heldin for providing PAE Rα cells and Dr. Bronek Pytowski for help with the Scatchard analysis.

References

1. Heldin CH, Ostman A, Ronnstrand L. Signal transduction via platelet-derived growth factor receptors. Biochim Biophys Acta 1998;1378:F79–113.

2. Li X, Ponten A, Aase K, et al. PDGF-C is a new protease-activated ligand for the PDGF α-receptor. Nat Cell Biol 2000;2:302–9.

3. Soriano P. The PDGF α receptor is required for neural crest cell development and for normal patterning of the somites. Development 1997;124:2691–700.

4. Heldin CH, Westermark B. Mechanism of action and *in vivo* role of platelet-derived growth factor. Physiol Rev 1999;79:1283–316.

5. Ostman A, Heldin CH. Involvement of platelet-derived growth factor in disease: development of specific antagonists. Adv Cancer Res 2001;80:1–38.

6. Henriksen R, Funa K, Wilander E, Backstrom T, Ridderheim M, Oberg K. Expression and prognostic significance of platelet-derived growth factor and its receptors in epithelial ovarian neoplasms. Cancer Res 1993;53:4550–4.

7. Fudge K, Wang CY, Stearns ME. Immunohistochemistry analysis of platelet-derived growth factor A and B chains and platelet-derived growth factor α and β receptor expression in benign prostatic hyperplasias and Gleason-graded human prostate adenocarcinomas. Mod Pathol 1994;7:549–54.

8. de Jong JS, van Diest PJ, van d, V, Baak JP. Expression of growth factors, growth inhibiting factors, and their receptors in invasive breast cancer. I. An inventory in search of autocrine and paracrine loops. J Pathol 1998;184:44–52.

9. Zhang P, Gao WY, Turner S, Ducatman BS. Gleevec (STI-571) inhibits lung cancer cell growth (A549) and potentiates the cisplatin effect *in vitro*. Mol Cancer 2003;2:1.

10. Hermanson M, Funa K, Hartman M, et al. Platelet-derived growth factor and its receptors in human glioma tissue: expression of messenger RNA and protein suggests the presence of autocrine and paracrine loops. Cancer Res 1992;52:3213–9.

11. Barnhill RL, Xiao M, Graves D, Antoniades HN. Expression of platelet-derived growth factor (PDGF)-A, PDGF-B and the PDGF-α receptor, but not the PDGF-β receptor, in human malignant melanoma *in vivo*. Br J Dermatol 1996;135:898–904.

12. Sulzbacher I, Traxler M, Mosberger I, Lang S, Chott A. Platelet-derived growth factor-AA and -α receptor expression suggests an autocrine and/or paracrine loop in osteosarcoma. Mod Pathol 2000;13:632–7.

13. Fleming TP, Saxena A, Clark WC, et al. Amplification and/or overexpression of platelet-derived growth factor receptors and epidermal growth factor receptor in human glial tumors. Cancer Res 1992;52: 4550 – 3.

14. Shawver LK, Slamon D, Ullrich A. Smart drugs: tyrosine kinase inhibitors in cancer therapy. Cancer Cell 2002;1:117 – 23.

15. George D. Targeting PDGF receptors in cancer—rationales and proof of concept clinical trials. Adv Exp Med Biol 2003;532:141 – 51.

16. LaRochelle WJ, Jensen RA, Heidaran MA, et al. Inhibition of platelet-derived growth factor autocrine growth stimulation by a monoclonal antibody to the human α platelet-derived growth factor receptor. Cell Growth Differ 1993;4:547 – 53.

17. Lokker NA, O'Hare JP, Barsoumian A, et al. Functional importance of platelet-derived growth factor (PDGF) receptor extracellular immunoglobulin-like domains. Identification of PDGF binding site and neutralizing monoclonal antibodies. J Biol Chem 1997;272:33037 – 44.

18. Eriksson A, Siegbahn A, Westermark B, Heldin CH, Claesson-Welsh L. PDGF α- and β-receptors activate unique and common signal transduction pathways. EMBO J 1992;11:543 – 50.

19. Harlow E, Lane D. Antibodies: a laboratory manual. Cold Spring Harbor (NY): Cold Spring Harbor Laboratory; 2004. p. 211 – 3.

20. de Haard HJ, van Neer N, Reurs A, et al. A large non-immunized human Fab fragment phage library that permits rapid isolation and kinetic analysis of high affinity antibodies. J Biol Chem 1999;274:18218 – 30.

21. Lu D, Jimenez X, Zhang H, Bohlen P, Witte L, Zhu Z. Selection of high affinity human neutralizing antibodies to VEGFR2 from a large antibody phage display library for antiangiogenesis therapy. Int J Cancer 2002;97: 393 – 9.

22. Lu D, Shen J, Vil MD, et al. Tailoring *in vitro* selection for a picomolar affinity human antibody directed against vascular endothelial growth factor receptor 2 for enhanced neutralizing activity. J Biol Chem 2003; 278:43496 – 507.

23. Burtrum D, Zhu Z, Lu D, et al. A fully human monoclonal antibody to the insulin-like growth factor I receptor blocks ligand-dependent signaling and inhibits human tumor growth *in vivo*. Cancer Res 2003;63:8912 – 21.

24. Duan DS, Pazin MJ, Fretto LJ, Williams LT. A functional soluble extracellular region of the platelet-derived growth factor (PDGF) β-receptor antagonizes PDGF-stimulated responses. J Biol Chem 1991; 266:413 – 8.

25. Heldin CH, Backstrom G, Ostman A, et al. Binding of different dimeric forms of PDGF to human fibroblasts: evidence for two separate receptor types. EMBO J 1988;7:1387 – 93.

26. Heidaran MA, Yu JC, Jensen RA, Pierce JH, Aaronson SA. A deletion in the extracellular domain of the α platelet-derived growth factor (PDGF) receptor differentially impairs PDGF-AA and PDGF-BB binding affinities. J Biol Chem 1992;267:2884 – 7.

27. Fleming TP, Matsui T, Heidaran MA, Molloy CJ, Artrip J, Aaronson SA. Demonstration of an activated platelet-derived growth factor autocrine pathway and its role in human tumor cell proliferation *in vitro*. Oncogene 1992;7:1355 – 9.

28. Nister M, Libermann TA, Betsholtz C, et al. Expression of messenger RNAs for platelet-derived growth factor and transforming growth factor-α and their receptors in human malignant glioma cell lines. Cancer Res 1988; 48:3910 – 8.

29. MacDonald TJ, Brown KM, LaFleur B, et al. Expression profiling of medulloblastoma: PDGFRA and the RAS/MAPK pathway as therapeutic targets for metastatic disease. Nat Genet 2001;29:143 – 52.

30. McGary EC, Weber K, Mills L, et al. Inhibition of platelet-derived growth factor-mediated proliferation of osteosarcoma cells by the novel tyrosine kinase inhibitor STI571. Clin Cancer Res 2002;8:3584 – 91.

31. Beckmann MP, Betsholtz C, Heldin CH, et al. Comparison of biological properties and transforming potential of human PDGF-A and PDGF-B chains. Science 1988;241:1346 – 9.

32. Heinrich MC, Corless CL, Duensing A, et al. PDGFRA activating mutations in gastrointestinal stromal tumors. Science 2003;299:708 – 10.

33. Fitzer-Attas CJ, Do MS, Feigelson S, Vadai E, Feldman M, Eisenbach L. Modification of PDGFα receptor expression or function alters the metastatic phenotype of 3LL cells. Oncogene 1997;15:1545 – 54.

34. Forsberg K, Valyi-Nagy I, Heldin CH, Herlyn M, Westermark B. Platelet-derived growth factor (PDGF) in oncogenesis: development of a vascular connective tissue stroma in xenotransplanted human melanoma producing PDGF-BB. Proc Natl Acad Sci U S A 1993;90:393 – 7.

35. Keating MT, Williams LT. Autocrine stimulation of intracellular PDGF receptors in v-*sis*-transformed cells. Science 1988;239:914 – 6.

36. Fleming TP, Matsui T, Molloy CJ, Robbins KC, Aaronson SA. Autocrine mechanism for v-*sis* transformation requires cell surface localization of internally activated growth factor receptors. Proc Natl Acad Sci U S A 1989;86:8063 – 7.

37. Uehara H, Kim SJ, Karashima T, et al. Effects of blocking platelet-derived growth factor-receptor signaling in a mouse model of experimental prostate cancer bone metastases. J Natl Cancer Inst 2003;95: 458 – 70.

38. Apte SM, Fan D, Killion JJ, FIJ. Targeting the platelet-derived growth factor receptor in antivascular therapy for human ovarian carcinoma. Clin Cancer Res 2004;10:897 – 908.

39. Hwang RF, Yokoi K, Bucana CD, et al. Inhibition of platelet-derived growth factor receptor phosphorylation by STI571 (Gleevec) reduces growth and metastasis of human pancreatic carcinoma in an orthotopic nude mouse model. Clin Cancer Res 2003;9:6534 – 44.

40. Peres R, Betsholtz C, Westermark B, Heldin CH. Frequent expression of growth factors for mesenchymal cells in human mammary carcinoma cell lines. Cancer Res 1987;47:3425 – 9.

41. Vignaud JM, Marie B, Klein N, et al. The role of platelet-derived growth factor production by tumor-associated macrophages in tumor stroma formation in lung cancer. Cancer Res 1994;54:5455 – 63.

42. Shao ZM, Nguyen M, Barsky SH. Human breast carcinoma desmoplasia is PDGF initiated. Oncogene 2000;19:4337 – 45.

43. Alvares O, Klebe R, Grant G, Cochran DL. Growth factor effects on the expression of collagenase and TIMP-1 in periodontal ligament cells. J Periodontol 1995;66:552 – 8.

44. Robbins JR, McGuire PG, Wehrle-Haller B, Rogers SL. Diminished matrix metalloproteinase 2 (MMP-2) in ectomesenchyme-derived tissues of the Patch mutant mouse: regulation of MMP-2 by PDGF and effects on mesenchymal cell migration. Dev Biol 1999;212:255 – 63.

45. Skobe M, Fusenig NE. Tumorigenic conversion of immortal human keratinocytes through stromal cell activation. Proc Natl Acad Sci U S A 1998;95:1050 – 5.

46. Bergers G, Song S, Meyer-Morse N, Bergsland E, Hanahan D. Benefits of targeting both pericytes and endothelial cells in the tumor vasculature with kinase inhibitors. J Clin Invest 2003;111:1287 – 95.

47. Pietras K, Rubin K, Sjoblom T, et al. Inhibition of PDGF receptor signaling in tumor stroma enhances antitumor effect of chemotherapy. Cancer Res 2002;62:5476 – 84.

Molecular Cancer Therapeutics

Targeting the platelet-derived growth factor receptor α with a neutralizing human monoclonal antibody inhibits the growth of tumor xenografts: Implications as a potential therapeutic target

Nick Loizos, Yan Xu, Jim Huber, et al.

Mol Cancer Ther 2005;4:369-379.